Volume 12 | Number 5 | 7 March 2025

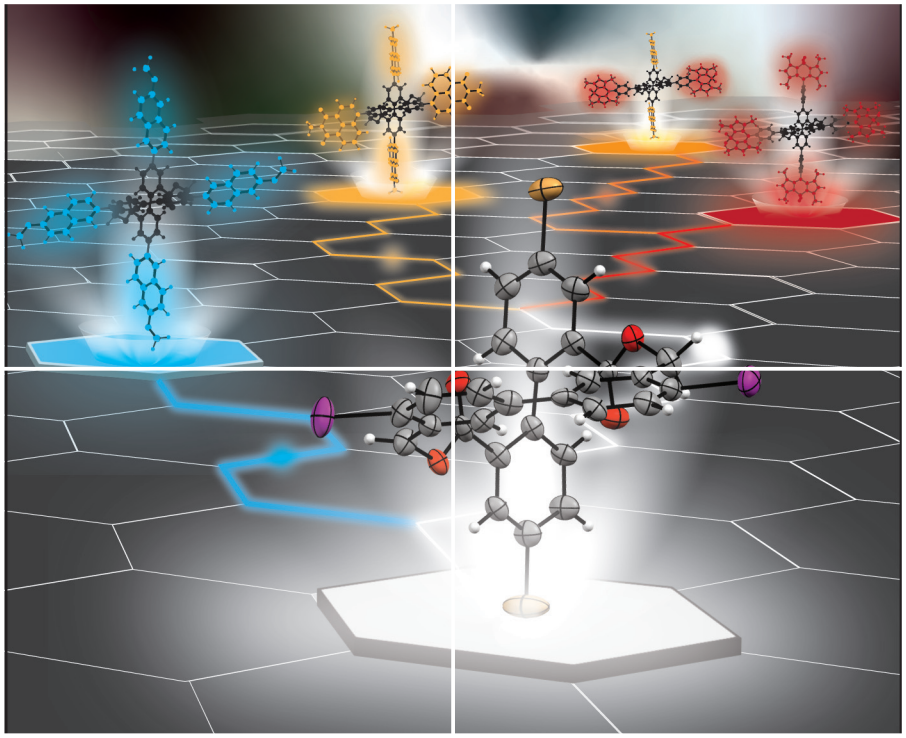

ORGANIC CHEMISTRY FRONTIERS

CCS 中国化学会 CHINESE CHEMICAL SOCIETY
SIOC 1950
ROYAL SOCIETY OF CHEMISTRY
rsc.li/frontiers-organic

ORGANIC CHEMISTRY FRONTIERS

RESEARCH ARTICLE

View Article Online
View Journal | View Issue

Check for updates

Cite this: *Org. Chem. Front.*, 2025, **12**, 1399

A cross-shaped organic framework: a multi-functional template arranging chromophores†

Camiel C. E. Kroonen, [a] Adriano D'Addio, [a] Allesandro Prescimone, [a] Daniel Häussinger [a] and Marcel Mayor *[a,b,c]

This work explores the use of a cross-shaped organic framework that is used as a template for the investigation of multi-functionalized chromophores. We report the design and synthesis of a universal cross-shaped building block bearing two bromines and two iodines on its peripheral positions. The template can be synthesized on a gram scale in a five-step reaction comprising an oxidative homo-coupling macro-cyclization. The formed scaffold was selectively functionalized *via* Suzuki cross-coupling reactions with methoxynaphthalene, naphthalimide and BODIPY derivatives, yielding a library of cross-shaped and chromophore-decorated model compounds, all of which were fully characterized. The formed racemic bis- and tetra-substituted crosses were resolved *via* chiral stationary phase HPLC, and assignment of the enantiomers was done *via* comparison of experimental and simulated electronic circular dichroism spectra as well as enantiomer single-crystal analysis. Additionally, the hybrid naphthalimide/BODIPY chromophore was found to be acting as an intramolecular Förster energy resonance transfer pair, which was investigated in more detail. With this easy-to-functionalize universal building block, we believe it might prove to be useful in the study of different sets of chromophores.

Received 26th September 2024,
Accepted 2nd December 2024

DOI: 10.1039/d4qo01808g

rsc.li/frontiers-organic

Open Access Article. Published on 04 December 2024. Downloaded on 5/28/2025 11:12:45 AM.
This article is licensed under a Creative Commons Attribution-NonCommercial 3.0 Unported Licence.

Introduction

Unravelling the chemistry and photophysics of dyes has occupied the scientific world from the time of discovering the first synthetic colorant about 150 years ago.[1] Ever since, prediction of and control over color and luminescence have become important due to the rising applications of dyes and pigments in our everyday life. To understand these apparent properties, scientist have studied the underlying processes that explain the features and characteristics of these optically active molecules.

Researchers found that the influence of two or more optically active molecules in close proximity can result in a variety of photophysical effects, *e.g.*, excimer-induced red shifts, aggregation-induced fluorescence, *etc.*[2,3] Understanding these phenomena proves to be critical due to their use in a variety of fields such as solar cells,[4,5] sensing,[6] catalysis[7,8] and biomedical studies,[9] for example, Förster Energy Resonance Transfer (FRET), which is used to study molecular dynamics in biological systems like substrate protein binding.[10] Here, the donor chromophore or fluorophore, when in close enough proximity, transfers its potential fluorescence light to the next chromophore (acceptor).[11] As a result, the overall fluorescence will vary depending on the distance and alignment between the donor and acceptor pair, providing insights into the spatial displacement and arrangement of the species *e.g.* molecular binding events. Understanding these photophysical phenomena, by studying how properties of distinct chromophores near each other influence one another, requires suitable model compounds with a fixed arrangement of their dye subunits.

Recently, there have been some examples investigating separated chromophores, attached to well-defined molecular superstructures.[12–15] Crassous and co-workers synthesized helicene conjugates with naphthalimide, porphyrin or diketopyrrolopyrrole (DPP) derivatives.[12–14] They showed that the chiral information of the helicenes was successfully transferred to the otherwise achiral optically active subunits. In addition, they showed that the measured circular dichroism directly relates to the exciton coupling between the

[a]*Department of Chemistry, University of Basel, St Johanns-Ring 19, Basel 4056, Switzerland. E-mail: Marcel.Mayor@unibas.ch; https://www.chemie1.unibas.ch/Bmayor/*
[b]*Institute for Nanotechnology (INT), Karlsruhe Institute of Technology (KIT), P. O. Box 3640, Karlsruhe 76021, Germany*
[c]*Lehn Institute of Functional Materials (LIFM), School of Chemistry, Sun Yat-Sen University (SYSU), Guangzhou 510275, China*

† Electronic supplementary information (ESI) available. CCDC 2378892–2378894. For ESI and crystallographic data in CIF or other electronic format see DOI: https://doi.org/10.1039/d4qo01808g

Open Access Article. Published on 04 December 2024. Downloaded on 5/28/2025 11:12:45 AM.
This article is licensed under a Creative Commons Attribution-NonCommercial 3.0 Unported Licence.

chromophores. Another work, by Sidler *et al.*, showed the importance of the spatial arrangement of chromophores by fixing a-chiral dyes (6-methoxy naphthalene) in a chiral structure.[16] The confined arrangement in space resulted in induced axial chirality based on the intramolecular Davydov splitting assignment of excimers.[17,18] Both studies showed how important the structural alignment of the chromophores is for the resulting properties of the system.

Inspired by these works and our recently developed cross-shaped motif, we envisioned that we could use this as a new organic superstructure. The rigid conformation of the cross-shaped motif, approaching close to a 90° angle, makes it a perfect candidate to supplement the already existing library of molecular frameworks.[19] To make this motif even more appealing, it consists of two thermally stable enantiomers. A particularly interesting feature broadening the playing field is that the rigid cross-shaped motif can be split into a pair of rigid rod-type subunits by cleavage of both ester bonds.[20]

Here, we present a universal cross-shaped building block consisting of a pair of rigid rods, which can easily be functionalized and distinguished by common cross-coupling protocols. A library of systems consisting of up to four chromophores, including an intramolecular FRET pair, was synthesized to demonstrate its potential. These new multi-chromophore model compounds were analyzed in terms of optical and chiro-optical properties, which were attributed to the variety of structural features the cross-shaped framework provides.

Results and discussion

Design and retrosynthesis

Our design principle is depicted in Fig. 1. The template consists of two biphenyls bridged over two esters, in 1-1′ and 2-2′, respectively, resulting in a cross-shaped conformation. We envisioned that functionalizing the peripheral positions with achiral chromophores would allow us to transfer the chiral information from the template to the chromophores and that we could investigate different sets of chromophores in close proximity. We opted for a set of three chromophores: the first being the 6-methoxynaphthalene chosen due to its well-studied optical and electronic properties as well as its previous use in a chiral architecture reported by our group.[16] The latter two – a naphthalimide (NI) derivative and a BODIPY (BY) derivative – were chosen due to their potential of forming an intramolecular (FRET) pair as the emission spectrum (λ_{em}) of the NI overlaps with the absorption spectrum (λ_{abs}) of the BODIPY.[21,22] The intention was to profit from the FRET experiment to demonstrate the cleavage of the template. As sketched in Fig. 1(d), a FRET is expected in the cross-shaped model compound, which should disappear upon template cleavage, liberating terminally NI and BODIPY decorated rigid rods.

In order to access a variety of cross-shaped tetrachromophores, we revised the synthetic route of our previous work. The original synthetic route contained a number of parallel sequences equal to the amount of different target compounds. In this work, we present a modular approach with a universal

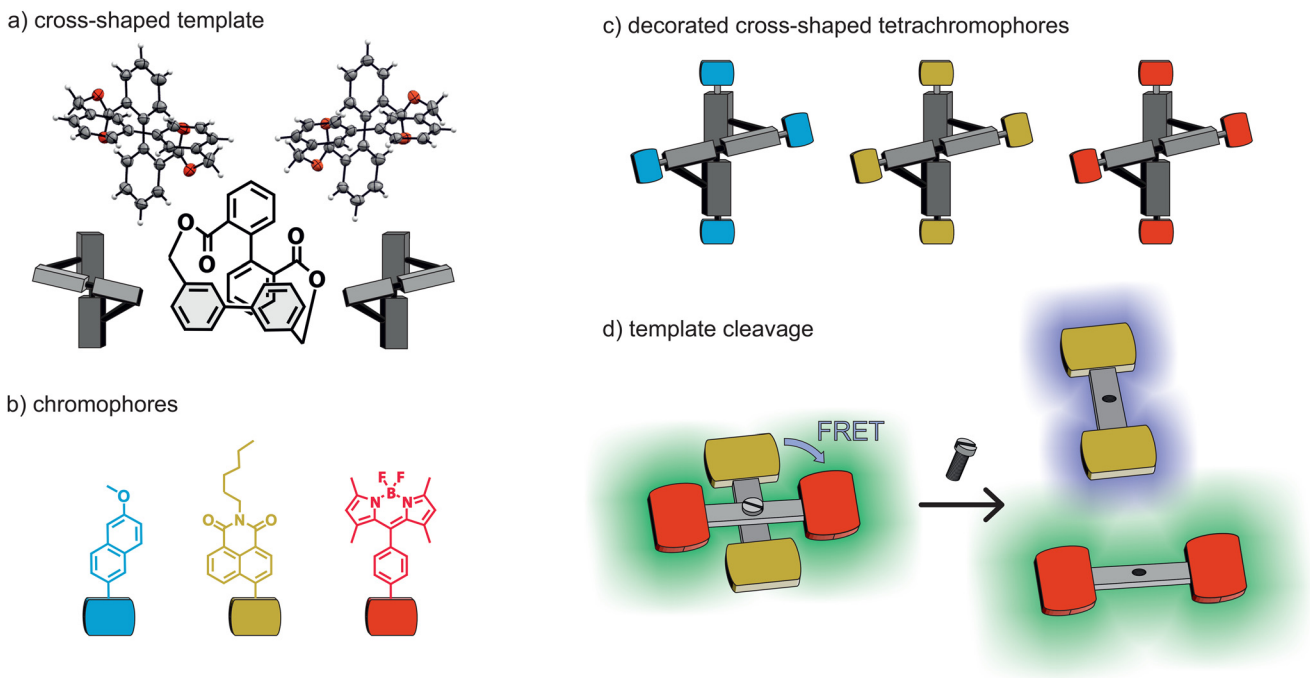

Fig. 1 Schematic representation of the functionalization of a cross-shaped molecule with chromophores to obtain a library of mono- or hybrid chromophores. (a) Cross-shaped motif consisting of both (*M*) and (*P*) conformers adopting a distorted tetrahedron conformation. (b) Target chromophores for functionalization. (c) Library of decorated cross-shaped tetrachromophores. (d) A hybrid chromophore showing intramolecular-FRET activity, which after template cleavage results in the liberation of two differently decorated rigid rods.

 This journal is © the Partner Organisations 2025

Open Access Article. Published on 04 December 2024. Downloaded on 5/28/2025 11:12:45 AM.
This article is licensed under a Creative Commons Attribution-NonCommercial 3.0 Unported Licence.

building block which can be decorated *via* well-established cross-coupling chemistry, like, for example, the Suzuki and Sonogashira reactions. This on one hand reduces the number of reaction steps significantly, and on the other hand, allows for the implementation of the bis-biphenyl cross template into a variety of molecular designs. The universal building block $\mathbf{C_{Br2I2}}$ is displayed in Scheme 1, while further insights concerning its design (ESI, Fig. S1†) and retrosynthesis (ESI, Scheme S1†) are provided in the ESI.† $\mathbf{C_{Br2I2}}$ contains iodide and bromide functionalities, acting as two separate addressable motifs at the end of both bars of the cross. The retrosynthetic analysis (displayed in the ESI, Scheme S1,† because it basically duplicates the forward synthesis displayed in Scheme 1) of $\mathbf{C_{Br2I2}}$ was envisioned over bis-boronic ester intermediate **1** *via* an oxidative homo-coupling and deprotection process, and the Sandmeyer sequence could be transformed into $\mathbf{C_{Br2I2}}$. **1** could be obtained from previously synthesized 4,4′-dibromo-diphenic acid **2** and boronic ester **3** *via* a two-fold esterification reaction.[19] After successful synthesis of $\mathbf{C_{Br2I2}}$, the more reactive aryl-iodide over aryl-bromide with regard to palladium-catalyzed cross-coupling chemistry enables the temperature-controlled sequential decoration with coupling partners and thus also the controlled assembly of the members of the library.[23]

Synthesis and characterization of $\mathbf{C_{Br2I2}}$

The preparation of $\mathbf{C_{Br2I2}}$, as depicted in Scheme 1, started with the Boc protection of (2-amino-5-bromophenyl)methanol **4** by a Boc anhydride in THF, followed by Miyaura borylation to yield **3** in good yields over two steps. Di-acid **2**, prepared as described in our previous work, was reacted with **3** *via* a two-fold Steglich esterification using *N*,*N*′-dicyclohexylcarbodiimide (DCC) and 4-dimethylaminopyridine (DMAP) to yield **1** in excellent yields.[19] The use of an excess amount of DCC (2 *vs.* 2.2 equiv.) turned out to be crucial, as the yield increased from a moderate level of 75% to almost a quantitative level of 95%. **1** was converted to $\mathbf{C_{Br2Boc2}}$ by applying palladium-catalyzed oxidative homo-coupling conditions. A slight modification of the solvent (THF *vs.* the toluene/MeOH mixture) improved the yield from ~50% to 65% for this key

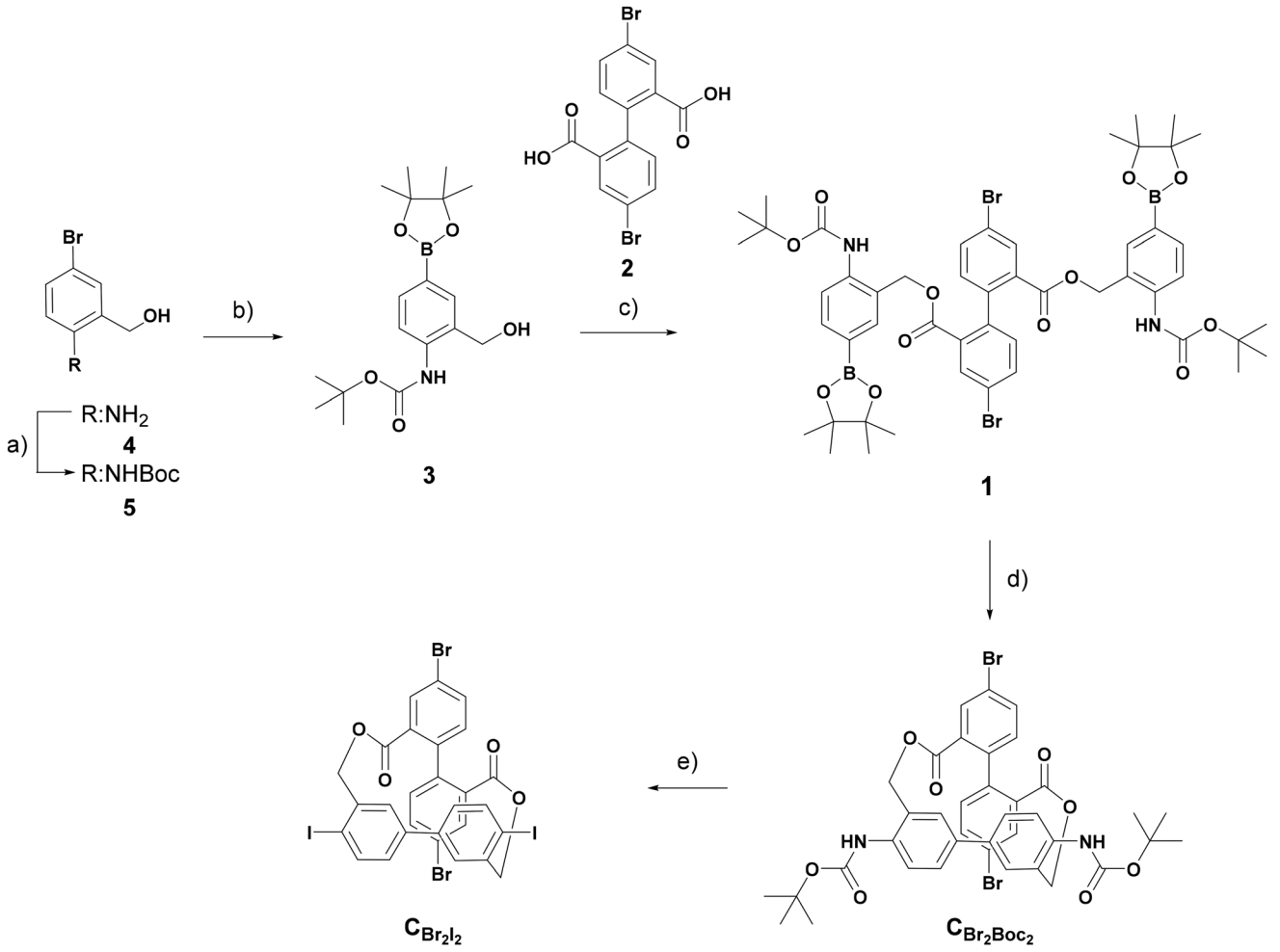

Scheme 1 Synthesis of $\mathbf{C_{Br2I2}}$. Conditions: (a) Boc_2O; DIPEA; THF; 0 °C–r.t.; 20 h; 66%. (b) $PdCl_2(dppf)$; B_2Pin_2; KOAc; dioxane; 85 °C; 22 h; 98%. (c) **2**; DCC; DMAP; CH_2Cl_2/DMF; r.t.; 16 h; 95%. (d) $PdCl_2(PPh_3)_2$; KF; $B(OH)_3$, Tol/MeOH/H_2O; r.t.; 16 h; 65%. (e) (i) p-TsOH; ACN/Tol; r.t./4 h; (ii) $NaNO_2$; KI; H_2O; –15 °C to r.t.; 1 h; 62%.

Open Access Article. Published on 04 December 2024. Downloaded on 5/28/2025 11:12:45 AM.
This article is licensed under a Creative Commons Attribution-NonCommercial 3.0 Unported Licence.

step. After the usual development on a small scale, these conditions were also applied on a multi-gram scale, accessing $\mathbf{C_{Br2Boc2}}$ in large quantities. In the final step, the Boc-protected amines were converted to iodine in a one-pot deprotection and Sandmeyer reaction using *para*-toluene sulfonic acid (*p*-TsOH) to obtain target $\mathbf{C_{Br2I2}}$. The one-pot strategy was chosen over the stepwise approach due to the instability of the free di-amine intermediate. A small optimization process showed that applying lower temperatures and the use of toluene as a co-solvent allowed the synthesis of the target in 62% isolated yield. The protocol allowed the gram-scale synthesis of $\mathbf{C_{Br2I2}}$ in 6 steps with an overall yield of 25% from commercial building blocks.

Structural analysis

The identity of $\mathbf{C_{Br2I2}}$ was corroborated by its solid-state structure (ESI, Fig. S34†). Single crystals suitable for X-ray analysis were obtained by slow vapor diffusion of MeOH into a solution of $\mathbf{C_{Br2I2}}$ in toluene. The solid-state structure analysis revealed the racemic mixture of both enantiomers (*M* and *P*). Interestingly the crystals organized themselves in a layered fashion, containing solely one of the enantiomers per alternating layer. The crystal structure also showed an angle between 80° and 86° between the two biphenyl moieties, which is in line with the previously reported structures.[19,20]

A study on the optical properties of the racemic mixture (*rac*)-$\mathbf{C_{Br2I2}}$ and its respective enantiomers (*M*)-$\mathbf{C_{Br2I2}}$ and (*P*)-$\mathbf{C_{Br2I2}}$ was conducted. The enantiomers were separated using chiral stationary phase HPLC (heptane : ethyl acetate 1 : 1, Chiralpak IG column), and circular dichroism (CD) was measured. The good separation (ESI, Fig. S2†) of (*rac*)-$\mathbf{C_{Br2I2}}$ allowed for preparative isolation of tens of milligrams of the enantiomers. The CD spectra of the pure enantiomers indicated opposite signs of the Cotton bands (ESI, Fig. S3†) and allowed *via* DFT calculations the assignment of the first eluting enantiomer to be (*M*)-$\mathbf{C_{Br2I2}}$, while the second being (*P*)-$\mathbf{C_{Br2I2}}$ (ESI, Fig. S4†). This was further corroborated by growing enantiopure crystals of the second eluting enantiomer (Fig. 2). Slow diffusion of MeOH into a solution of E2-$\mathbf{C_{Br2I2}}$ rendered single crystals suitable for X-ray analysis, which were resolved as bearing only *P* enantiomers. Due to the fact that the obtained Flack parameter is nearly 0, the absolute configuration can be assigned with certainty and thus identifies the second eluting enantiomer as (*P*)-$\mathbf{C_{Br2I2}}$.

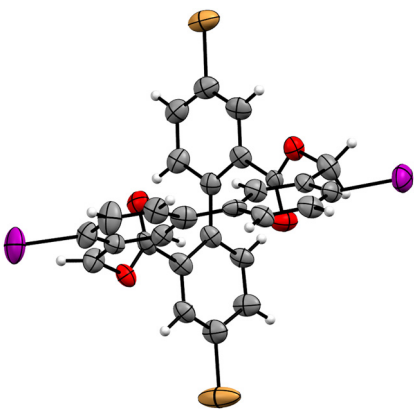

Fig. 2 Solid-state structure of enantiopure (*P*)-$\mathbf{C_{Br2I2}}$ plotted as an ORTEP plot with 50% probability, obtained as a second eluting enantiomer.

Selective chromophore decoration

With $\mathbf{C_{Br2I2}}$ in hand, a library of cross-shaped tetrachromophores was synthesized, as depicted in Scheme 2. At first the bis- and tetra-functionalized methoxynaphthalenes ($\mathbf{C_{Br2Naph2}}$ and $\mathbf{C_{Naph4}}$), were synthesized *via* either a stepwise approach over $\mathbf{C_{Br2Chromophore2}}$ or a direct four-fold Suzuki reaction. $\mathbf{C_{Br2I2}}$ was reacted in the presence of 2 equivalents of commercially available 6-methoxynaphthalene boronic acid (**Naph-B(OH)$_2$**), yielding $\mathbf{C_{Br2Naph2}}$ in good yields. $\mathbf{C_{Naph4}}$ could in its turn be obtained from $\mathbf{C_{Br2Naph2}}$ in the same catalytic system by simply adding an additional 2 equivalents of **Naph-B(OH)$_2$** and elevating the temperature to 85 °C. Alternatively, $\mathbf{C_{Br2I2}}$ was reacted at 85 °C with 4 equivalents of **Naph-(BOH)$_2$** to yield the four-fold substituted $\mathbf{C_{Naph4}}$ in one step from $\mathbf{C_{Br2I2}}$.

To access the naphthalimide (**NI**) and BODIPY (BY) functionalized model compounds, the corresponding literature known boronic ester coupling partners were synthesized (ESI, Page S6 and S7†).[24,25] **NI-Br** and BY-**Br** were synthesized *via* imide condensation and a one-pot condensation process, oxidation and a BF_2 insertion reaction, respectively. The bromides were converted to boronic esters *via* a Miyaura borylation process, yielding **NI-Bpin** and BY-**Bpin** in good yields over two steps.

The corresponding bis- and tetra-functionalized chromophores ($\mathbf{C_{Br2NI2}}$, $\mathbf{C_{NI4}}$, $\mathbf{C_{Br2BY2}}$ and $\mathbf{C_{BY4}}$) as well as a hybrid system ($\mathbf{C_{NI2BY2}}$) were synthesized following the same pathway as the methoxynaphthalene chromophores (Scheme 2). Depending on the solubility of the involved reaction partners and target structures, the solvent mixtures were adapted, yielding all of the desired cross-shaped and chromophore-decorated targets after simple silica gel column chromatography in acceptable yields and good quality. The quick accessibility of the variety of cross-shaped tetrachromophores showcases the easy and selective peripheral decoration of $\mathbf{C_{Br2I2}}$ *via* the common Suzuki cross-coupling protocols. Of particular interest was the subsequent optical investigation of the obtained chromophore-decorated model compounds.

Physicochemical analysis

Optical analysis. All cross-shaped tetrachromophores were characterized *via* absorption and fluorescence spectroscopy, as shown in Fig. 3 and Table S1.† Comparison of the absorption spectra between the two- and four-fold decorated crosses, respectively, showed in all cases the not-surprising increase of absorptivity in the spectral region associated with the absorption of the particular chromophore, namely methoxynaphthalene (300 nm), naphthalimide (360 nm) or BODIPY (500 nm). Upon comparison of the fluorescence spectra, it was seen that only the set of crosses with the **Naph** chromophores exhibited

 This journal is © the Partner Organisations 2025

Open Access Article. Published on 04 December 2024. Downloaded on 5/28/2025 11:12:45 AM.
This article is licensed under a Creative Commons Attribution-NonCommercial 3.0 Unported Licence.

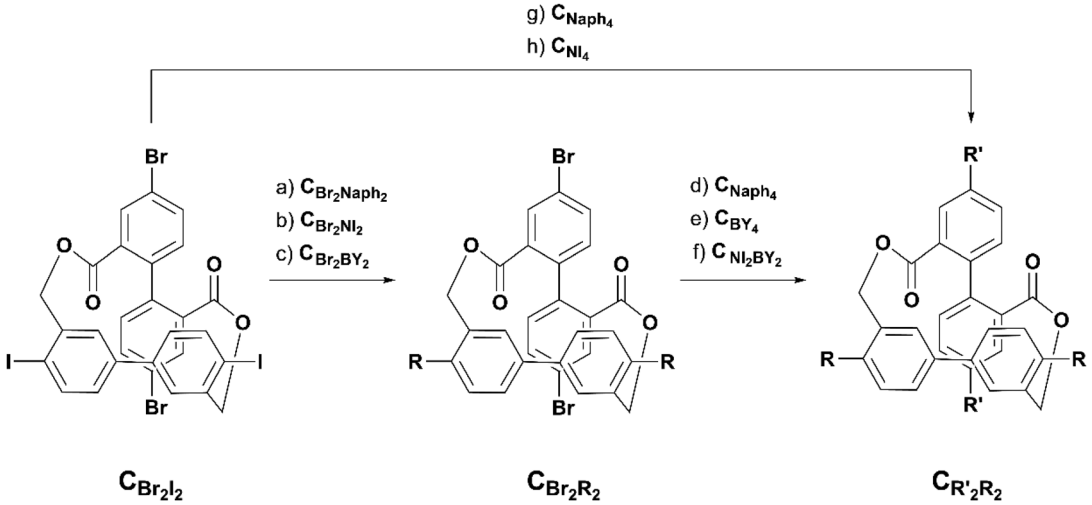

Scheme 2 Synthesis of $C_{Br2Naph2}$, C_{Naph4}, C_{Br2NI2}, C_{NI4}, C_{Br2BY2}, C_{BY4}, and C_{NI2BY2}. Reagents and conditions: (a) **Naph-BOH$_2$**; $PdCl_2$(dppf); K_2CO_3; THF/H_2O (4 : 1); 4.5 h; 55 °C; 80%; (b) **NI-BPin**; $PdCl_2$(dppf); K_2CO_3; THF/H_2O (4 : 1); 4.5 h; 55 °C; 61%; (c) BY-**BPin**; $PdCl_2$(dppf); K_2CO_3; THF/H_2O (4 : 1); 4.5 h; 55 °C; 90%; (d) $C_{Br2Naph2}$; **Naph-BOH$_2$**; $PdCl_2$(dppf); K_2CO_3; dioxane/H_2O (4 : 1); 24 h; 85 °C; 47%; (e) C_{Br2BY2}; BY-**BPin**; dioxane/H_2O (4 : 1); 24 h; 90 °C; 21%; (f) C_{Br2BY2}; **NI-BPin**; dioxane/DMF/H_2O (9 : 1 : 2.5); 16 h; 90 °C; 61%; (g) **Naph-BOH$_2$**; $PdCl_2$(dppf); K_2CO_3; dioxane/H_2O (4 : 1); 20 h; 85 °C; 56%; (h) **NI-BPin**; $PdCl_2$(dppf); K_2CO_3; Tol/EtOH/H_2O (4 : 1 : 1); 18 h; 85 °C; 27%.

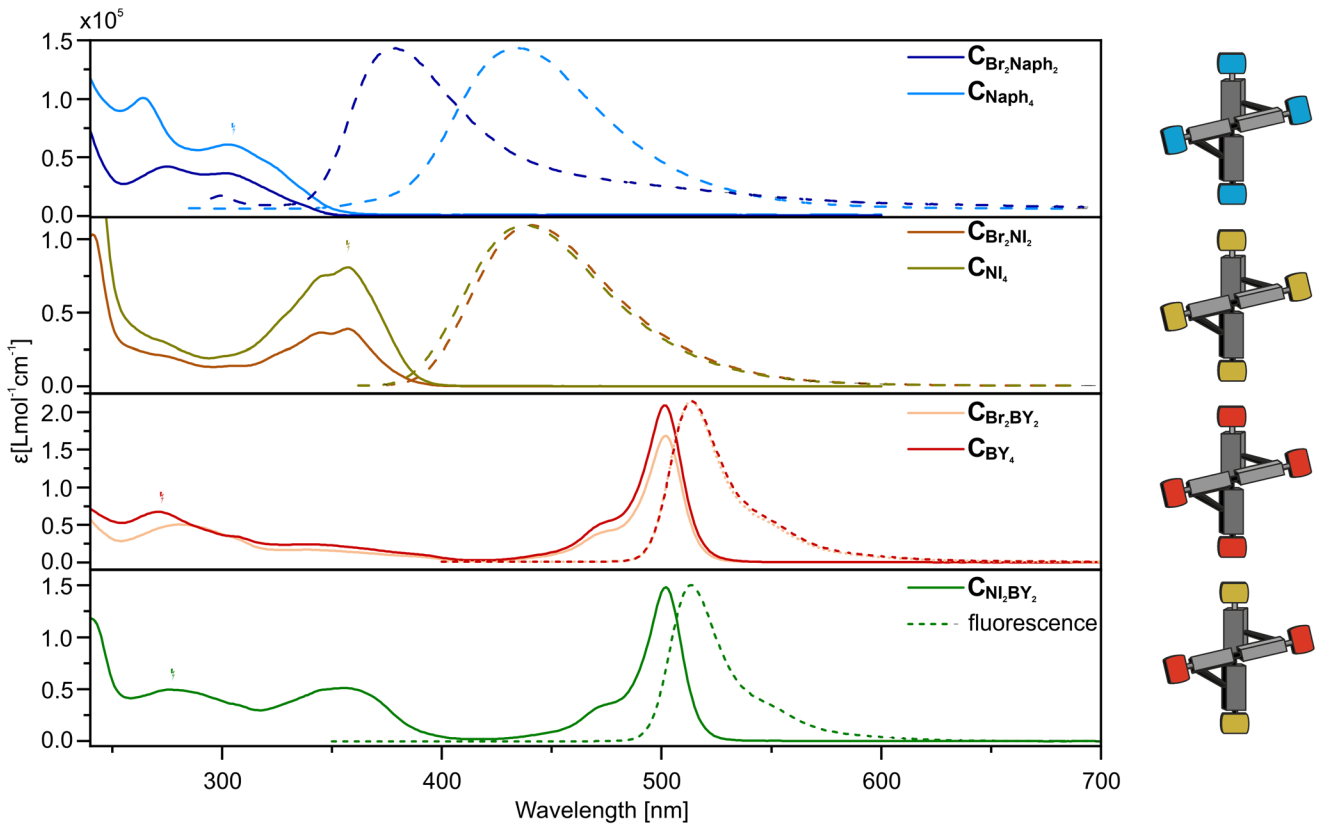

Fig. 3 Absorption spectra (solid line) and fluorescence spectra (dashed line) of $C_{Br2Naph2}$ and C_{Naph4} (blue), C_{Br2NI2} and C_{NI4} (yellow), C_{Br2BY2} and C_{BY4} (red), and C_{NI2BY2} (green) in CH_2Cl_2. All spectra were recorded at 20 °C; c ~10^{-6} mol L^{-1} for absorption and c ~10^{-7} mol L^{-1} for emission.

a large bathochromic shift, from 378 nm for $C_{Br2Naph2}$ to 432 nm for C_{Naph4}. This shift can be rationalized by the conjugation of the electron-donating methoxynaphthalene with the electron-withdrawing ester of the core when substituted on the bromine position. While substitution on the iodine position does not provide any conjugation with a withdrawing group,

Open Access Article. Published on 04 December 2024. Downloaded on 5/28/2025 11:12:45 AM.
This article is licensed under a Creative Commons Attribution-NonCommercial 3.0 Unported Licence.

yielding comparable fluorescence maxima with earlier reported structures having the same methoxynaphthalene motifs.[26,27] The almost non-existing fluorescence shift in the **NI** and BY decorated crosses can be explained by the isolation of the chromophores due to their more demanding steric nature twisting their π-system out of plane with respect to the bi-phenyl rod and the absence of significant exciton coupling. Telfer *et al.* correlated the magnitude of the coupling between two perpendicular dipoles and reported that this coupling almost disappears when approaching a 90° angle, as observed in the here-reported (almost 90°) cross-shaped model compounds.[28]

By comparing the spectra of $\mathbf{C_{NI2BY2}}$ with the **NI** and BY series, the absorbance features of both chromophores at 360 and 500 nm, respectively, can clearly be identified. The fluorescent spectrum of $\mathbf{C_{NI2BY2}}$, however, has solely a BY characteristic with the exact same emission maxima ($\lambda_{em,max}$ = 513 nm) as the other BY decorated model compounds. Even excitation of $\mathbf{C_{NI2BY2}}$ at 360 nm, which is the main **NI** absorption band, results in the same BY fluorescence spectra (ESI, Fig. S11†). As the emission of **NI** overlaps with the absorption region of BY, this is the expected optical feature of an intramolecular FRET, further corroborating the close proximity of both chromophores in the structure.

Structural analysis. With the library of chromophore-decorated crosses in hand, their structural conformation was analyzed. To our delight, we were able to grow single crystals suitable for the X-ray analysis of $\mathbf{C_{Br2BY2}}$ (Fig. 4). Slow evaporation of heptane into a solution of $\mathbf{C_{Br2BY2}}$ in a toluene–CH_2Cl_2 mixture rendered bright red crystals. The X-ray structure analysis revealed an *I*2/*a* space group, where the unit cell consisted of a mixture of one *M* enantiomer and one *P* enantiomer. One can see that the BODIPY motif is twisted with respect to its phenyl spacer, resulting from the steric repulsion of the methyl groups. Furthermore, the center part of the molecule exhibits the earlier seen almost 90° cross shape between the two rods of the molecule.

As we continued our structural investigation, we quickly encountered the complexity of these systems in terms of nomenclature and supposed chirality assignment. The difference in the substitution pattern on rod 1 (*ortho*) and rod 2 (*meta*) induces a size mismatch similar to banister type molecules, hence we describe the arising helicity with *P* and *M*.‡[29] In Fig. 5, a schematic representation of the structure is displayed, with the corresponding nomenclature of the cross-shaped framework, acting as a guide for the following part.

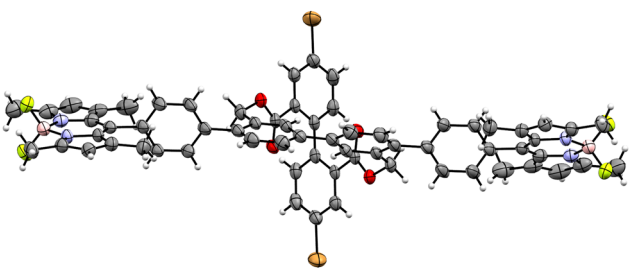

Fig. 4 Solid-state structure of (*M*)-$\mathbf{C_{Br2BY2}}$ in the racemic crystal of $\mathbf{C_{Br2BY2}}$, plotted as ORTEP plots with 50% probability. Plotted as a single enantiomer and without solvent molecules for clarity.

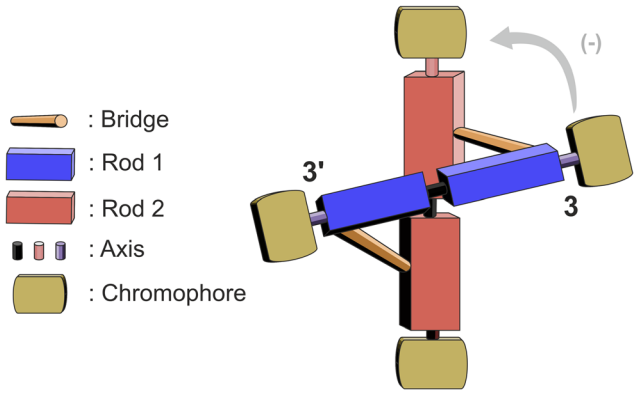

Fig. 5 Schematic representation of the (*P*)-cross-shaped framework decorated with four chromophores. **Rod 1** resembles the alcohol side of the molecule, while **Rod 2** the ester side.

Analysis by ^{1}H NMR spectroscopy revealed that the **Naph**- and BY-decorated crosses showed the characteristic peak splitting of the diastereotopic benzylic ester protons into two doublets (ESI, Page S75–S116†). However, in the case of the **NI** series ($\mathbf{C_{Br2NI2}}$ and $\mathbf{C_{NI4}}$), according to our interpretation, a set of eight doublets was found (ESI, Fig. S16†). In contrast, when **NI** was introduced on **rod 2** ($\mathbf{C_{NI2BY2}}$), this was not observed.

We attributed this additional splitting to the presence of two additional conformational orientations of the bulkier **NI** in comparison with the **Naph** and phenyl spacers of BY. The steric repulsion of the CH_2 bridge at the peripheral 3 and 3′ positions of **rod 1** in combination with the rigid center motif forces the **NI** moiety to an additional set of conformers. Due to the hindered rotation of **NI**, 2 additional atropisomeric centers were created: R_{a3}/S_{a3} and $R_{a3'}/S_{a3'}$.

Using VT-NMR, we investigated the rotational barrier of $\mathbf{C_{Br2NI2}}$ (Fig. S17†). To our surprise, upon heating to 120 °C in $C_2D_2Cl_4$, we saw minor shifts in the proton signals, but the diastereotopic protons remained visible as 8 doublets. This points at a surprisingly high rotation barrier for the conformer interconversion. We hypothesize that this might arise from the structural entanglement of the center motif. As the **NI** motif clashes with the ester bridge on both sides simultaneously, the center motif probably cannot adopt the conformation required to let the **NI** pass.

To further shed light on the potential different conformers, DFT calculations were performed. The geometry optimized structures revealed that there were 4 potential conformers per enantiomer (ESI, Page S20 and Fig. S43–S45†), namely $R_{a3},R_{3'}$; $S_{a3},S_{a3'}$; $R_{a3},S_{a3'}$ and $S_{a3},R_{a3'}$. In these calculated structures, the $R_{a3},S_{a3'}$ and $S_{a3},R_{a3'}$ conformers are identical, giving a total of 3

‡ The chirality could also be described by axial or planar chirality. In general, the *P* isomer of the crosses corresponds to an R_a,R_a or S_P configuration.

This journal is © the Partner Organisations 2025

Open Access Article. Published on 04 December 2024. Downloaded on 5/28/2025 11:12:45 AM.
This article is licensed under a Creative Commons Attribution-NonCommercial 3.0 Unported Licence.

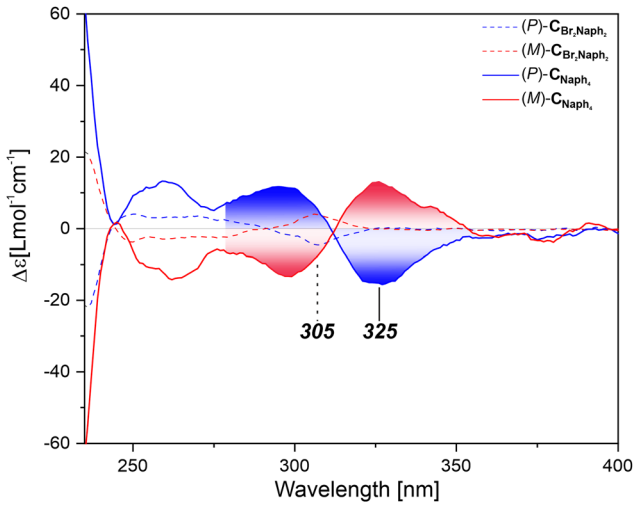

Fig. 6 ECD spectra of the (blue) (*P*) and (red) (*M*) enantiomers of $\mathbf{C_{Br2Naph2}}$ (dashed line) and $\mathbf{C_{Naph4}}$ (solid line). Bisignate signals of $\mathbf{C_{Naph4}}$ are displayed by the integrated area under the respective plots.

diastereoisomers; thus, 3 pairs of doublets would be expected. Instead, 4 pairs of doublets were observed (ESI, Fig. S16†), suggesting that, for the R_{a3},$S_{a3'}$ (=S_{a3},$R_{a3'}$) conformer, there is a symmetry loss. Thus, assuming that the chemical shielding for R_{a3} and $R_{a3'}$ as well as for S_{a3} and $S_{a3'}$ are identical or very close would lead to additional signal splitting, hence the additional set of doublets.

To gain further comprehension about the elaborate architecture, their chiral properties were studied by comparing the recorded spectra with the simulated ones. First, the enantiomers of all chromophore-decorated cross-shaped model compounds were separated using analytical scale chiral-stationary phase HPLC (ESI, Page S18, S22, S25 and S27†). In the case of $\mathbf{C_{Br2NI2}}$ and $\mathbf{C_{NI4}}$, the focus was on the separation of the (*M*) and (*P*) enantiomers. However, the HPLC traces (ESI, Fig. S18†) revealed that the enantiomers were indeed composed of several conformers. With in-line CD detection, the conformation of the center motif was assigned, assuring that the enantiomer sets were successfully separated (ESI, Page S22†). To corroborate this claim experimentally, enantiopure syntheses of (*P*)-$\mathbf{C_{Br2NI2}}$ and (*P*)-$\mathbf{C_{NI4}}$ were performed with (*P*)-$\mathbf{C_{Br2I2}}$ as the starting material. The samples obtained by the enantiopure assembly were identical to the separated ones from racemic synthesis, assuring the enantiopurity of the separated samples.

With all separated enantiomers in hand, their respective CD spectra were recorded (ESI, Page S18, S23, S25 and S27†). As expected, moderate Cotton bands of opposite sign were observed for all here-reported separated pairs of enantiomers. Simulation of all *P* isomers and comparison to the experimental spectra allowed the assignment of the helicity of all the resolved samples. With the here-applied separation conditions, the *P* isomers elute first during the resolution of $\mathbf{C_{Br2Naph2}}$, $\mathbf{C_{Br2NI2}}$, and $\mathbf{C_{Naph4}}$; they elute second in the case of $\mathbf{C_{Br2I2}}$, $\mathbf{C_{Br2BY2}}$, $\mathbf{C_{NI4}}$, $\mathbf{C_{BY4}}$ and $\mathbf{C_{NI2BY2}}$.

As an example, the CD spectra of the enantiomers of the **Naph** series are displayed in Fig. 6. Upon comparison of the CD spectra recorded for the two- and four-fold substituted chromophores, $\mathbf{C_{Br2Naph2}}$ and $\mathbf{C_{Naph4}}$, respectively, a significant red shift in the spectra was observed. While the first Cotton band of $\mathbf{C_{Br2Naph2}}$ appeared at 305 nm, it was at 325 nm in the case of $\mathbf{C_{Naph4}}$. This shift can be assigned to the communication between the methoxynaphthalene subunits on **rod 1** and **rod 2**, respectively, as it is absent when only **rod 1** is substituted. The observed bisignate signal for the $\mathbf{C_{Naph4}}$ enantiomers indicates an exciton coupled feature.[18] Comparison of the CD signal to the earlier reported methoxynaphthalene architecture of Sidler *et al.* showed that these specific Cotton bands appear at exactly the same wavelengths, strengthening the argument for an exciton coupled signal.[16] Inspired by this observation, we applied the exciton chirality method (ECM) to the four-fold decorated crosses: $\mathbf{C_{Naph4}}$, $\mathbf{C_{NI4}}$ and $\mathbf{C_{BY4}}$.

The orientation of **rod 1** to **rod 2** in the *P* isomers should lead to a so-called negative couplet, as indicated by the grey arrow in Fig. 5. This negative couplet was indeed observed in (*P*)-$\mathbf{C_{Naph4}}$, (*P*)-$\mathbf{C_{NI4}}$, and (*P*)-$\mathbf{C_{BY4}}$ (ESI, Fig. S31†), while in the case of the *M* enantiomers, the bisignate signal was first positive and then negative, hence, a positive couplet.

While $\mathbf{C_{Br2Naph2}}$ and $\mathbf{C_{Br2NI2}}$ lack this feature, $\mathbf{C_{Br2BY2}}$ showed a weaker but clear bisignate signal at around 500 nm. A positive couplet was observed for the *P* enantiomer, while the *M* enantiomer displayed a negative one. Obviously, in the case of $\mathbf{C_{Br2BY2}}$, the chiral information is communicated over **rod 1** rather than between the terminal chromophores of both rods of the scaffold. Our current working hypothesis is that this is only detected for the BY chromophore because of the orientation of the excited dipole moment with a substantial contribution perpendicular to the rod's main axis, which is not the case for the other two chromophores. As the bi-phenyl axis of **rod 1** is entangled with the helicity of the central part of the cross (adopting an R_a configuration‡), a positive couplet is expected for the *P* enantiomer (ESI, Fig. S32†).

According to the here-presented results, the ECM method is suited to assign the respective enantiomers for their four-fold substituted chromophores; however, the careful consideration of all chiral centers turned out to be crucial. The created library allowed us to dive into initially unexpected features, which *via* full-geometrical examination could be assigned to a variety of features the framework exhibits.

FRET system. To explore the FRET activity of $\mathbf{C_{NI2BY2}}$, the template was cleaved in order to liberate the **NI** and BY decorated rods, respectively, as displayed in Fig. 7. Exposure of the chromophore to an aq. LiOH solution in THF/MeOH yielded overnight a change in the fluorescence signal visible by the bare eye from bright green to light faded blue. After acidic work-up, the cleaved pair of rods was dissolved in CH_2Cl_2, and fluorescence spectroscopy resolved two distinct emission peaks at 426 nm and 513 nm, respectively. As a control experiment, a reference sample of $\mathbf{C_{NI2BY2}}$ was stirred with NaCl instead of LiOH. As displayed in Fig. 7, the reference sample displayed exclusively emission at 513 nm, and the successful

Open Access Article. Published on 04 December 2024. Downloaded on 5/28/2025 11:12:45 AM.
This article is licensed under a Creative Commons Attribution-NonCommercial 3.0 Unported Licence.

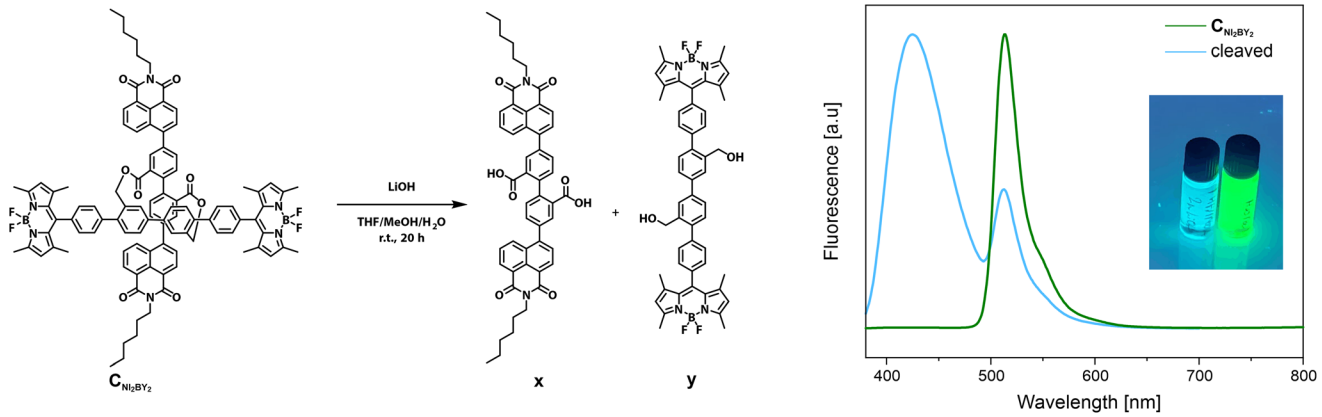

Fig. 7 Cleavage of the ester template of $\mathbf{C_{NI2BY2}}$ by exposure to LiOH, resulting in the fluorescence change. (left) Reaction conditions of the transformation of $\mathbf{C_{NI2BY2}}$ to yield **NI-x** and **BY-y**. (right) Fluorescence spectrum, in CH_2Cl_2 at 20 °C, of $\mathbf{C_{NI2BY2}}$ (green) and the crude product after cleavage (blue); λ_{ex} (360 nm); (image) reaction mixture after the reaction (left) and reference with NaCl instead of LiOH (right) under a 366 nm UV lamp.

cleavage could easily be accessed by comparing the reaction mixtures under a UV lamp (inset in Fig. 7). Furthermore, to verify that the reaction conditions do not cause changes in the terminal chromophores, $\mathbf{C_{NI4}}$ and $\mathbf{C_{BY4}}$ were cleaved under identical conditions (ESI, Fig. S33†). Comparison of the cleaved reaction mixtures revealed that there were no changes in the fluorescence behavior of $\mathbf{C_{NI4}}$ and $\mathbf{C_{BY4}}$ upon cleavage, with a remaining deep blue-purple fluorescence for $\mathbf{C_{NI4}}$ and a bright green fluorescence for $\mathbf{C_{BY4}}$. The analysis of the fluorescence spectra showed for both cases a single emission peak, which are in agreement with the fluorescence spectra of the non-cleaved precursors ($\mathbf{C_{NI4}}$ and $\mathbf{C_{BY4}}$). The cleavage behaviour analysed by fluorescence spectroscopy corroborates the establishment of an intramolecular FRET pair in the cross-shaped architecture and demonstrates the potential of this template analyzing chromophores in a close confined space.

Conclusions

In conclusion, an organic cross-shaped framework is designed that acts as a template superstructure for the synthesis of (chiral) multi-chromophore architectures. A universal macrocyclic building block is synthesized on a gram scale that due to steric restrictions adopts a cross shape. The framework bears four attachment points that are used to selectively mount methoxynaphthalene, naphthalimide and BODIPY derivatives. The reactivity difference of aryl-iodine and aryl-bromine ensured the synthesis of a library of bi- and tetra-functionalized chromophores, including a hybrid intra-molecular FRET pair. NMR spectroscopy and (chiro)-optical analysis were conducted for all compounds and revealed in support of DFT calculations the geometrical configuration of the reported compounds. This was further supported by enantiopure solid-state structure analysis ($\mathbf{C_{Br2I2}}$) and the exciton chirality method ($\mathbf{C_{R4}}$). Lastly, removal of the template results in breaking the FRET pair of the hybrid chromophore ($\mathbf{C_{NI2BY2}}$), visualized by a change in its fluorescence properties.

The study shows that the organic framework acts as an excellent and versatile platform for studying a variety of chromophores in a confined space, allowing for the investigation of novel properties such as chirality and FRET. In addition, the presented halide-decorated precursor enables its integration as a functional unit in a variety of applications by C–C coupling chemistry.

Author contributions

C. C. E. K. conceptualized the project, performed the synthesis, characterized the compounds and wrote the manuscript; A. D'A. performed the DFT calculations and wrote the manuscript; A. P. analyzed the solid-state structures; D. H. performed the VT-NMR experiments; M. M. supervised the work and wrote the manuscript. All authors commented on the manuscript.

Data availability

The data supporting this article have been included as part of the ESI.† The crystallographic data for this paper can be found under the deposition number 2378892 for (*rac*)-$\mathbf{C_{Br2I2}}$, 2378893 for (*P*)-$\mathbf{C_{Br2I2}}$ and 2378894 for (*rac*)-$\mathbf{C_{Br2BY2}}$.† These data are provided by the joint Cambridge Crystallographic Data Centre and Fachinformations-zentrum Karlsruhe Access Structures service.

Conflicts of interest

There are no conflicts to declare.

This journal is © the Partner Organisations 2025

Open Access Article. Published on 04 December 2024. Downloaded on 5/28/2025 11:12:45 AM.
This article is licensed under a Creative Commons Attribution-NonCommercial 3.0 Unported Licence.

Acknowledgements

We thank Tim Henri Eggenweiler for his assistance in measuring quantum yield and fluorescence lifetime. We thank Aristide Coynel for his help during part of the synthesis. Generous support from the Swiss National Science Foundation (SNF) is acknowledged (200020_207744). M. M. acknowledges support from the 111 project (90002-18011002).

References

1 S. Benkhaya, S. M'rabet and A. El Harfi, A review on classifications, recent synthesis and applications of textile dyes, *Inorg. Chem. Commun.*, 2020, **115**, 107891.
2 A. Nitti and D. Pasini, Aggregation-Induced Circularly Polarized Luminescence: Chiral Organic Materials for Emerging Optical Technologies, *Adv. Mater.*, 2020, **32**, 1908021.
3 Q. Luo, L. Li, H. Ma, C. Lv, X. Jiang, X. Gu, Z. An, B. Zou, C. Zhang and Y. Zhang, Deep-Red fluorescence from isolated dimers: a highly bright excimer and imaging in vivo, *Chem. Sci.*, 2020, **11**, 6020–6025.
4 V. Saravanan, S. Ganesan and P. Rajakumar, Synthesis and DSSC application of BODIPY decorated triazole bridged and benzene nucleus cored conjugated dendrimers, *RSC Adv.*, 2020, **10**, 18390–18399.
5 I. Jinchu, C. O. Sreekala and K. S. Sreelatha, Dye Sensitized Solar Cell Using Natural Dyes as Chromophores, *Mater. Sci. Forum*, 2014, **771**, 39–51.
6 T. Schembri, L. Kolb, M. Stolte and F. Würthner, Polarized, color-selective and semi-transparant organic photodiode of aligned merocyanine H-aggregates, *J. Mater. Chem. C*, 2024, **12**, 4948–4953.
7 M. Gryszel, T. Schlossarek, F. Würthner, M. Natali and E. D. Głowacki, Water-Soluble Cationic Perylene Diimide Dyes as Stable Photocatalysts for H_2O_2 Evolution, *ChemPhotoChem*, 2023, **7**, e202300070.
8 S. Wang, Z. Xie, D. Zhu, S. Fu, Y. Wu, H. Yu, C. Lu, P. Zhou, M. Bonn, H. I. Wang, Q. Liao, H. Xu, X. Chen and C. Gu, Efficient photocatalytic production of hydrogen peroxide using dispersible and photoactive porous polymers, *Nat. Commun.*, 2023, **14**, 6891.
9 J. Li, Z. Zhuang, X. Lou, Z. Zhao and B. Z. Tang, Molecular Design and Biomedical Application of AiEgens with Photochemical Activity, *Chem. Biomed. Imaging*, 2023, **1**, 785–795.
10 D. Shrestha, A. Jenei, P. Nagy, G. Vereb and J. Szöllősi, Understanding FRET as a Research Tool for Cellular Studies, *Int. J. Mol. Sci.*, 2015, **16**, 6718–6756.
11 B. R. Masters, Paths to Förster's resonance energy transfer (FRET) theory, *Eur. Phys. J. H*, 2014, **39**, 87–139.
12 P. Josse, L. Favereau, C. Shen, S. Dabos-Seignon, P. Blanchard, C. Cabanetos and J. Crassous, Enantiopure versus Racemic Naphtaimide End-Capped Helicenic Non-Fullerene Electron Acceptors: Impact on Organic Phorovoltaics Performance, *Chem. – Eur. J.*, 2017, **23**, 6277–6281.
13 K. Dhbaibi, P. Matozzo, L. Abella, M. Jean, N. Vanthuyne, J. Autschbach, L. Favereau and J. Crassous, Exciton coupling chirality in helicene-porphyrin conjugates, *Chem. Commun.*, 2021, **57**, 10743–10746.
14 K. Dhbaibi, L. Favereau, M. Srebro-Hooper, M. Jean, N. Vanthuyne, F. Zinna, B. Jamoussi, L. D. Bari, J. Autschbach and J. Crassous, Exciton coupling in diketo-pyrrolopyrorole-helicene derivatives leads to red an near-infrared circularly polarized luminescence, *Chem. Sci.*, 2018, **9**, 735–742.
15 H. Langhals, A. Hofer, S. Bernhard, J. S. Siegel and P. Mayer, Axially Chiral Bichromophoric Fluorescent Dyes, *J. Org. Chem.*, 2011, **76**, 990–992.
16 E. Sidler, J. Malinčík, A. Prescimone and M. Mayor, Induced axial chirality by a tight belt: naphtalene chromophores fixed in a 2,5-substituted cofacial para-phenylene-ethynylene framework, *J. Mater. Chem. C*, 2021, **9**, 16199–16207.
17 N. Harada and K. Nakanishi, Exciton chirality method and its application to configurational and conformational studies of natural products, *Acc. Chem. Res.*, 1972, **5**, 257–263.
18 N. J. Hestand and F. C. Spano, Expanded Theory of H- and J-Molecular Aggregates: The Effects of Vibronic Coupling and Intermolecular Charge Transfer, *Chem. Rev.*, 2018, **118**, 7069–7163.
19 C. C. E. Kroonen, A. D'Addio, A. Prescimone, O. Fuhr, D. Fenske and M. Mayor, A Cross-Shaped Monomer as Building Block for Molecular Textiles, *Helv. Chim. Acta*, 2023, **106**, e202200204.
20 C. C. E. Kroonen, A. Hinaut, A. D'Addio, A. Prescimone, D. Häussinger, G. Navarro-Marín, O. Fuhr, D. Fenske, E. Meyer and M. Mayor, Towards Molecular Textiles: Synthesis and Characterization of Molecular Patches, *Chem. – Eur. J.*, 2024, e202402866.
21 L. Yu, Y. Xu, J. Kim, J. Lee and J. S. Kim, A rational design of AIE-active fluorophore for the fingerprint optical detection, *Bull. Korean Chem. Soc.*, 2023, **44**, 516–522.
22 Í. A. O. Bozzi, L. A. Machado, E. B. T. Diogo, F. G. Delolo, L. O. F. Barros, G. A. P. Graça, M. H. Araujo, F. T. Martins, L. F. Pedrosa, L. C. da Luz, E. S. Moraes, F. S. Rodembusch, J. S. F. Guimarães, A. G. Oliveira, S. H. Röttger, D. B. Werz, C. P. Souza, F. Fantuzzi, J. Han, T. B. Marder, H. Braunschweig and E. N. da Silva Júnior, Electrochemical Diselenation of BODIPY Fluorophores for Bioimaging Applications and Sensitization of 1O2, *Chem. – Eur. J.*, 2024, **30**, e202303883.
23 L. M. Bannwart, T. Müntener, M. Rickhaus, L. Jundt, D. Häussinger and M. Mayor, Bicyclic Phenyl-Ethynyl Architectures: Synthesis of a 1,4-Bis(phenylbuta-1,3-diyn-1-yl) Benzene Banister, *Chem. – Eur. J.*, 2021, **27**, 6295–6307.
24 M. Xu, J.-M. Han, Y. Zhang, X. Yang and L. Zang, A selective fluorescence turn-on sensor for trace vapor detection of

Open Access Article. Published on 04 December 2024. Downloaded on 5/28/2025 11:12:45 AM.
This article is licensed under a Creative Commons Attribution-NonCommercial 3.0 Unported Licence.

hydrogen peroxide, *Chem. Commun.*, 2013, **49**, 11779–11781.

25 J. Zhai, T. Pan, J. Zhu, Y. Xu, J. Chen, Y. Xie and Y. Qin, Boronic Acid Functionalized Boron Dipyrromethene Fluorescent Probes: Preparation, Characterization, and Sacharides Sensing Applications, *Anal. Chem.*, 2012, **84**, 10214–10220.

26 G. M. Rodriguez-Muñiz, M. Gomez-Mendoza, E. Nuin, I. Andreu, M. L. Marin and M. A. Miranda, "Snorkelling" vs. "diving" in mixed micelles probed by means of a molecular bathymeter, *Org. Biomol. Chem.*, 2017, **15**, 10281–10288.

27 L. J. Martínez and J. C. Scaiano, Characterization of the Transient Intermediates Generated from the Photoexcitation of Nabumetone: A Comparison with Naproxen, *Photochem. Photobiol.*, 1998, **68**, 646–651.

28 S. G. Telfer, T. M. McLean and M. R. Waterland, Excition coupling in coordination compounds, *Dalton Trans.*, 2011, **40**, 3097–3108.

29 A. D'Addio, J. Malinčik, O. Fuhr, D. Fenske, D. Häussinger and M. Mayor, Geländer Molecules with Orthogonal Joints: Synthesis of Macrocyclic Dimers, *Chem. – Eur. J.*, 2022, **28**, e202201678.

This journal is © the Partner Organisations 2025